Available online at www.sciencedirect.com
ScienceDirect
Tetrahedron
Tetrahedron 64 (2008) 549–558
www.elsevier.com/locate/tet

Conformational and self-assembly studies of helix forming hexapeptides containing two α-amino isobutyric acids

Anita Dutt [a], Michael G.B. Drew [b], Animesh Pramanik [a,*]

[a] Department of Chemistry, University of Calcutta, 92, A.P.C. Road, Kolkata 700 009, India
[b] School of Chemistry, The University of Reading, Whiteknights, Reading RG6 6AD, UK

Received 20 July 2007; received in revised form 16 October 2007; accepted 1 November 2007
Available online 7 November 2007

Abstract

Single crystal X-ray diffraction studies reveal that three hexapeptides with general formula Boc–Ile–Aib–Xx–Ile–Aib–Yy–OMe, where Xx and Yy are Leu in peptide **I**, Leu and Phe in peptide **II**, and Phe and Leu in peptide **III**, respectively, adopt equivalent conformations that can be described as mixed 3_{10}/α-helice with two $4\rightarrow1$ and two $5\rightarrow1$ intramolecular N–H···O=C H-bonds. The peptides do not generate any helix-terminating Schellman motif despite having Aib at the penultimate position from C-terminus. In the crystalline state, the helices are packed in head-to-tail fashion through intermolecular hydrogen bonds to create supramolecular helical structures. The CD studies of the three hexapeptides in acetonitrile indicate that they are folded in well-developed 3_{10}-helical structures. NMR studies of peptide **I** in $CDCl_3$ also suggest the formation of a homogeneous 3_{10}-helical structure. The field emission scanning electron microscopic (FE-SEM) images of peptide **II** in the solid state reveal a non-twisted ribbon-like morphology, which is formed through lateral association of non-twisted filaments.

Keywords: Peptide; α-Amino isobutyric acid; 3_{10}-Helix; α-Helix; Ribbons

1. Introduction

There has been considerable discussion in the literature on the nature of the helical conformations adopted by Aib-rich sequences.[1–4] Both 3_{10}- and α-helical conformations have been characterized depending upon peptide length, sequence, and Aib content. The 3_{10}-helix is a structure stabilized by successive $4\rightarrow1$ CO···NH hydrogen bonds, with idealized φ and ψ values of $-60°$ and $-30°$ characteristic of the right-handed screw. The α-helix is stabilized by successive $5\rightarrow1$ hydrogen bonds with idealized φ and ψ values of $-55°$ and $-45°$ for a right-handed structure. The distinctions between these two helical types are subtle and involve very small changes in φ and ψ values. The conformational interconversion between 3_{10}- and α-helix can be easily achieved and has been the subject of several investigations.[5] Although various designed peptides have been reported the minimal peptide length required for stabilization of the α-helix relative to the 3_{10}-helix in Aib-containing peptides is still not unequivocally established.

Several studies with hexapeptides containing Aib have been reported in the literature.[2] It has been observed that hexapeptides with more than two Aib residues (≥50%) generally adopt well defined 3_{10}-helical structures in the crystalline state. Table 1, which includes all the reported hexapeptides with two Aib residues, shows that the first two hexapeptides (entries 1 and 2) exhibit 3_{10}-helical conformations, while the next two hexapeptides (entries 3 and 4) exhibit mixed 3_{10}/α-helical structures with the 3_{10} segment occurring at the N-terminus.[3] The notable difference is that unlike the first two hexapeptides, the second two peptides contain achiral Aib at the penultimate position from the C-terminus. Although Aib at this position generally helps to generate the helix-terminating Schellman motif through the formation of a $6\rightarrow1$ intramolecular hydrogen bond,[4,6] the third hexapeptide on the list (entry 3) does not produce any such motif. Another important difference is that the hexapeptides of mixed 3_{10}/α-helical conformations (entries 3 and 4) contain Pro in their sequences, which is not

* Corresponding author. Tel.: +91 33 2484 1647; fax: +91 33 2351 9755.
E-mail address: animesh_in2001@yahoo.co.in (A. Pramanik).

0040-4020/$ - see front matter © 2007 Elsevier Ltd. All rights reserved.
doi:10.1016/j.tet.2007.11.016

Table 1
Crystal structures of hexapeptide helices containing two Aib residues

Entry	Sequence	No. of H-bonds	Structure	Reference
1.	Boc–Ala–Leu–Aib–Ala–Leu–Aib–OMe·H_2O	3 (4→1)	3_{10}	3a
2.	L-Pro–L-Leu–Aib–Aib–L-Glu–L-Val–OH	2 (4→1)	3_{10}	3b
3.	Piv–Pro–Pro–Aib–Leu–Aib–Phe–OMe			
	Molecule A	4 (4→1)	Mixed $3_{10}/\alpha$	3c
		3 (5→1)		
	Molecule B	3 (4→1)		
		4 (5→1)		
4.	Boc–Pro–Aib–Gly–Leu–Aib–Leu–OMe	4 (4→1)	Mixed $3_{10}/\alpha$ (Schellman motif)	3d
		3 (5→1)		
		1 (6→1)		
5.	Boc–Ile–Aib–Leu–Ile–Aib–Leu–OMe (**I**)	2 (4→1)	Mixed $3_{10}/\alpha$	This work
		2 (5→1)		
6.	Boc–Ile–Aib–Leu–Ile–Aib–Phe–OMe (**II**)	2 (4→1)	Mixed $3_{10}/\alpha$	This work
		2 (5→1)		
7.	Boc–Ile–Aib–Phe–Ile–Aib–Leu–OMe (**III**)	2 (4→1)	Mixed $3_{10}/\alpha$	This work
		2 (5→1)		

generally observed in regular natural right-handed α-helices. Nevertheless, these two peptides indicate that hexapeptides with less than three Aib residues can show some small degree of α-helical character. Therefore, further studies are necessary with hexapeptides to assess the preferences between the 3_{10} and the α-helix conformations and also to assess the possibility of the formation of the Schellman motif.

In this context, we chose a set of three hexapeptides **I**–**III**, Boc–Ile–Aib–Xx–Ile–Aib–Yy–OMe, where Xx and Yy are Leu in peptide **I**, Leu and Phe in peptide **II**, and Phe and Leu in peptide **III**, respectively (Fig. 1). All the peptides **I**–**III** incorporate achiral Aib residue at the penultimate position and do not contain the helix-breaking Pro. So far, the Schellman motif has been characterized crystallographically only in peptide helices containing at least seven residues apart from the one hexapeptide (entry 4) included in Table 1. Therefore, the present study will provide insights into the occurrence of the Schellman motif in Aib-containing hexapeptides and also the preferred helical conformations. Peptides **I**–**III** were synthesized using conventional solution phase methodology (Scheme 1) and their solid-state structures and crystal packing were determined by X-ray diffraction analysis. The peptide conformations in the solution phase were probed by CD and NMR studies.

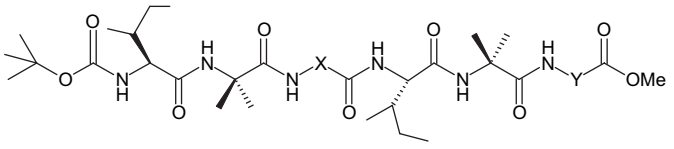

Figure 1. Schematic representation of peptides **I**–**III**. Peptide **I**: X=–CH–CH_2–CH–$(CH_3)_2$, Y=–CH–CH_2–CH–$(CH_3)_2$; peptide **II**: X=–CH–CH_2–CH–$(CH_3)_2$, Y=–CH–CH_2–Ph; peptide **III**: X=–CH–CH_2–Ph, Y=–CH–CH_2–CH–$(CH_3)_2$.

Apart from the conformational interest, the cylindrical helical structures readily generated in Aib-rich sequences are likely to find many novel applications in material science. Relevant reports include the synthesis of monodisperse liquid crystalline peptides based on Aib-containing helices[7] and the formation of self-assembling chiral monolayers of helical peptides bound to gold surfaces, in which immobilization is achieved by side chain thioether interaction.[8] Aib-containing helical peptides may be employed to assemble fibrils of various morphologies. In this report, field emission scanning

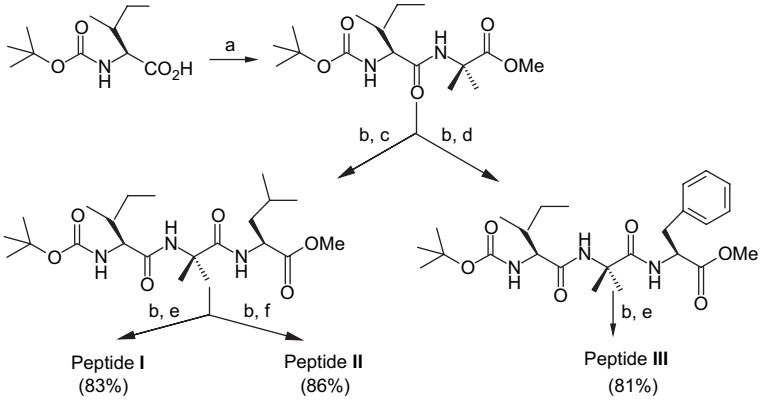

Scheme 1. Reagents and conditions: (a) DCM, H–Aib–OMe, DCC, HOBt, 0 °C, 90% yield; (b) MeOH, 2 M, NaOH, 80% yield; (c) DMF, H–Leu–OMe, DCC, HOBt, 0 °C, 90% yield; (d) DMF, H–Phe–OMe, DCC, HOBt, 0 °C, 95% yield; (e) DMF, Boc–IUL–OMe, CF_3COOH, 8 h, 0 °C; DMF, H–IUL–OMe, DCC, HOBt, 0 °C; (f) DMF, Boc–IUF–OMe, CF_3COOH, 8 h, 0 °C; DMF, H–IUL–OMe, DCC, HOBt, 0 °C.

electron microscopy (FE-SEM) has been employed to investigate the morphological properties of the peptides in the solid state.

2. Results and discussion

2.1. Single crystal X-ray diffraction studies

All the three peptides **I**–**III** crystallized with one molecule in the crystallographic asymmetric unit. Figures 2–4 illustrate the observed conformations of the peptides and demonstrate their similarities, while Tables 2 and 3 list the backbone torsion angles and the inter- and intramolecular hydrogen bonding dimensions, respectively. In peptide **I** the backbone torsion angles for residues 1, 2, and 5 lie in the helical ($3_{10}/\alpha_R$) region of the Ramachandran map. The φ and ψ values at residues 3 [−98.2(5)° and 7.9(6)°] and 4 [−104.6(5)° and −53.5(6)°] deviate significantly from the idealized values of helical ($3_{10}/\alpha_R$) region (Fig. 2, Table 2). Inspection of the hydrogen bonding parameters listed in Table 3 reveals that the molecule is stabilized by four intramolecular hydrogen bonds. Hexapeptide **I** adopts a mixed $3_{10}/\alpha$-helix conformation with two 4→1 intramolecular hydrogen bonds at the N-terminal and two 5→1 at the C-terminal. The Ile(1)CO is involved in bifurcated intramolecular hydrogen bonding with HN–Ile(4) (4→1) and HN–Aib(5) (5→1). As a result the backbone torsion angles (φ and ψ) at Leu(3) and Ile(4) deviate significantly from the helical region ($3_{10}/\alpha_R$) of the Ramachandran plot (Table 2). Interestingly, despite having achiral Aib at the penultimate position, peptide **I** does not generate the helix-terminating Schellman motif through a 6→1 intramolecular hydrogen bond at the C-terminal, which is commonly observed in peptide helices, which have lengths of seven residues or greater.

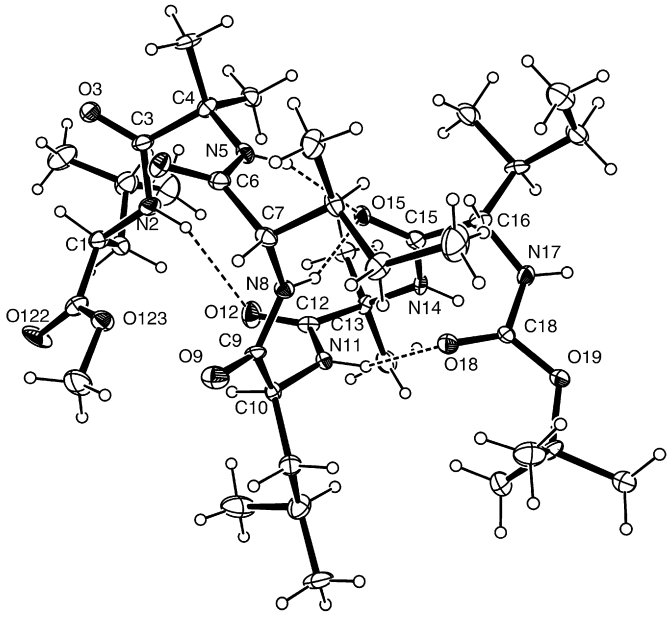

Figure 2. The ORTEP diagram of peptide **I** including atom numbering scheme. Thermal ellipsoids are shown at the level of 25% probability. Hydrogen bonds are shown as dotted lines.

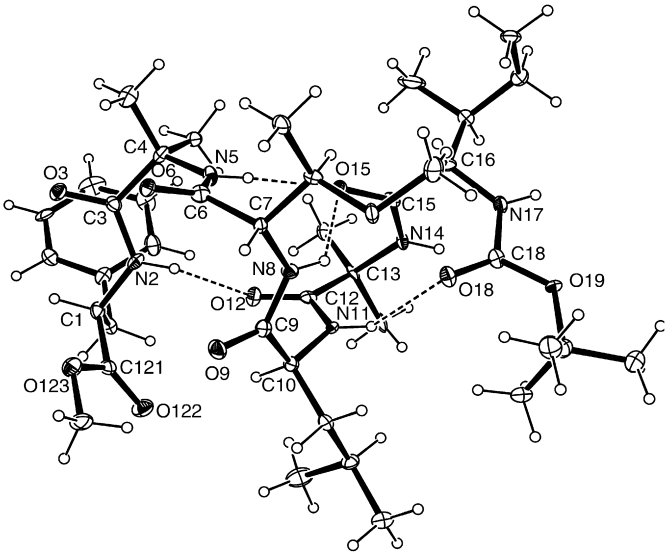

Figure 3. The ORTEP diagram of peptide **II** including atom numbering scheme. Thermal ellipsoids are shown at the level of 25% probability. Hydrogen bonds are shown as dotted lines.

Peptide **II** where the last residue, Leu(6), of peptide **I** has been replaced by Phe also shows a similar mixed $3_{10}/\alpha$-helical conformation without Schellman motif (Fig. 3, Table 2). The result shows that positioning Phe after the penultimate Aib in peptide **II** sequence does not help in Schellman motif formation. Peptide **III**, which incorporates Phe at the middle of the sequence also shows similar structural preferences to peptides **I** and **II** (Fig. 4, Table 2).

The crystal packing arrangements of peptides **I**–**III** are shown in Figure 5 (with side chains). Both peptides **I** and **II** crystallize in space group $P2_1$ but there are no hydrogen bonds between molecules related by the screw axis. Instead, peptides **I** and **II** are packed in head-to-tail fashion through intermolecular hydrogen bonds (Table 3) between the Aib(2)–

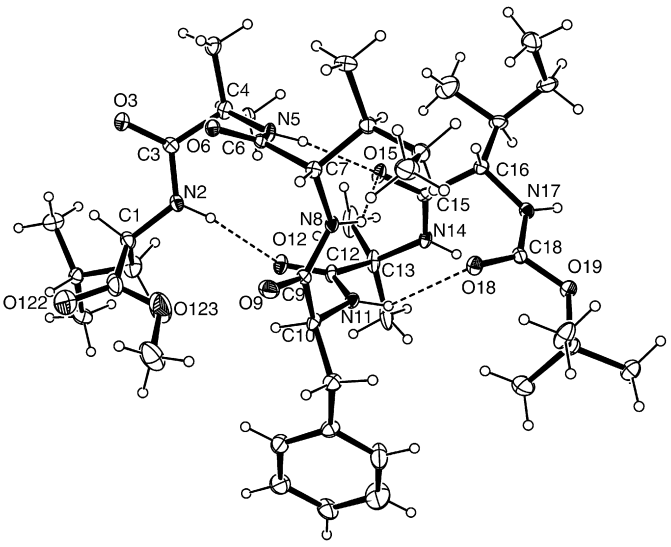

Figure 4. The ORTEP diagram of peptide **III** including atom numbering scheme. Thermal ellipsoids are shown at the level of 25% probability. Hydrogen bonds are shown as dotted lines.

Table 2
Selected backbone torsions (°) of peptides **I**–**III**

Residues	φ	ψ	ω
Peptide **I**			
Ile(1)	−50.4(6)	−39.7(6)	−179.8(4)
Aib(2)	−50.2(6)	−41.1(6)	−178.3(4)
Leu(3)	−98.2(5)	7.9(6)	−173.2(4)
Ile(4)	−104.6(5)	−53.5(6)	171.8(4)
Aib(5)	−57.2(6)	−43.0(5)	172.5(4)
Leu(6)	−129.0(5)	−179.8(5)	−167.4(5)
Peptide **II**			
Ile(1)	−48.1(7)	−43.2(6)	−179.2(4)
Aib(2)	−49.7(6)	−47.2(6)	−173.3(4)
Leu(3)	−90.1(6)	−11.2(7)	−169.0(5)
Ile(4)	−76.1(6)	−45.3(6)	169.9(4)
Aib(5)	−63.5(6)	−39.5(6)	171.5(5)
Phe(6)	−132.9(5)	−96.9(7)	−174.1(5)
Peptide **III**			
Ile(1)	−56.8(4)	−34.3(4)	−175.1(3)
Aib(2)	−51.8(5)	−44.4(5)	−174.5(3)
Phe(3)	−92.0(4)	0.7(5)	−172.7(3)
Ile(4)	−81.7(4)	−52.2(4)	161.8(3)
Aib(5)	−52.6(5)	−50.3(4)	176.9(3)
Leu(6)	−117.4(4)	148.3(5)	−165.4(3)

Table 3
Hydrogen bonding parameters of peptides **I**–**III**

D–H···A	H···A (Å)	D···A (Å)	D–H···A (°)
Peptide **I**			
Intramolecular			
Boc–CO···HN–Leu(3)	2.22	2.95(1)	143
Ile(1)–CO···HN–Ile(4)	2.12	2.93(1)	156
Ile(1)–CO···HN–Aib(5)	2.10	2.91(1)	157
Aib(2)–CO···HN–Leu(6)	2.57	3.21(1)	133
Intermolecular			
Aib(2)–NH···OC–Ile(4)[a]	2.06	2.90(1)	165
Peptide **II**			
Intramolecular			
Boc–CO···HN–Leu(3)	2.38	3.09(1)	141
Ile(1)–CO···HN–Ile(4)	2.45	3.07(1)	130
Ile(1)–CO···HN–Aib(5)	2.19	3.05(1)	176
Aib(2)–CO···HN–Phe(6)	2.27	2.94(1)	135
Intermolecular			
Aib(2)–NH···OC–Ile(4)[a]	2.09	2.93(1)	161
Peptide **III**			
Intramolecular			
Boc–CO···HN–Phe(3)	2.44	3.15(1)	140
Ile(1)–CO···HN–Ile(4)	2.27	2.95(1)	136
Ile(1)–CO···HN–Aib(5)	2.08	2.94(1)	172
Aib(2)–CO···HN–Leu(6)	2.30	3.05(1)	145
Intermolecular			
Boc–NH···OC–Aib(5)[b]	2.20	3.00	159
Aib(2)–NH···OC–Ile(4)[b]	2.15	3.00	167

[a] Symmetry elements: $x-1$, y, z.
[b] Symmetry elements: $x+y$, $-x$, $z-1/3$.

NH moiety of one molecule with the Ile(4)CO moiety of another molecule (symmetry element $x-1$, y, z) to create supramolecular helical structures along the crystallographic axis a. Peptide **III** crystallizes in space group $P3_1$ and by contrast with **I** and **II** the molecule forms two intermolecular hydrogen bonds between Boc–NH···OC–Aib(5) and Aib(2)–NH···OC–Ile(4) related by the 3_1 screw axis.

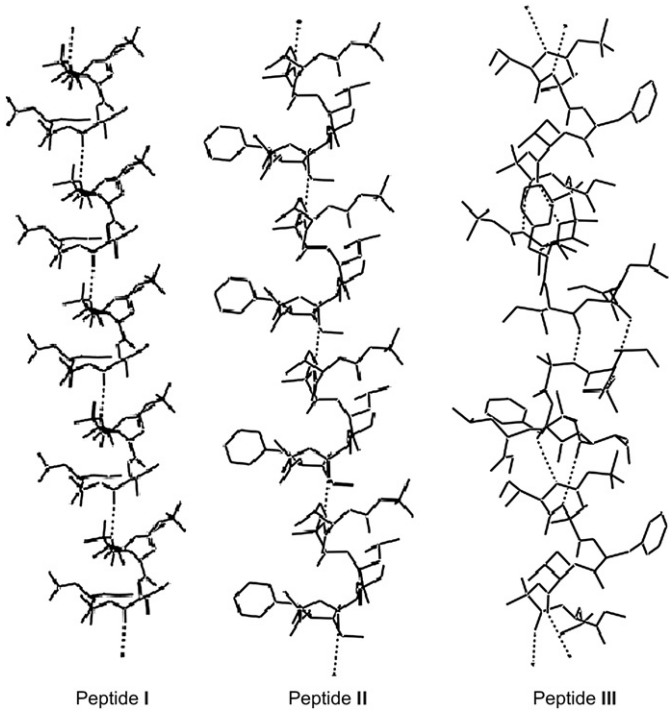

Figure 5. Packing diagrams of peptides **I**–**III** showing the formation of supramolecular helices. Intermolecular hydrogen bonds are indicated by dotted lines. Peptides **I** and **II** show one hydrogen bond between molecules related by translational symmetry along the *a* axis while peptide **III** shows two hydrogen bonds between adjacent molecules around the 3_1 screw axis.

2.2. Solution conformational analysis

Complete ^{1}H NMR assignments of peptide **I** were obtained using a combination of 2D COSY and ROESY methods in $CDCl_3$. In order to investigate the existence of intramolecular hydrogen bonding and peptide conformation in the solution phase, the solvent dependence of the NH chemical shifts was examined by NMR titration.[4a,9] In this experiment, a solution of the peptide in non-polar $CDCl_3$ (10 mM in 0.5 ml) was gradually titrated against polar $(CD_3)_2SO$. The changes in the chemical shifts are presented in Figure 6. The solvent titration experiment shows that by increasing the percentage of $(CD_3)_2SO$ in $CDCl_3$ from 0 to 14% (v/v) the net changes in the chemical shift ($\Delta\delta$) values for Ile(1)–NH, Aib(2)–NH, Leu(3)–NH, Ile(4)–NH, Aib(5)–NH, and Leu(6)–NH are 0.82, 0.50, 0.10, 0.17, 0.08, and 0.25 ppm, respectively. From the $\Delta\delta$ values, it is evident that Ile(1) and Aib(2) NH are solvent exposed, while the remaining NH groups at Leu(3), Ile(4), Aib(5) ,and Leu(6) are solvent shielded, indicating their involvement in intramolecular hydrogen bonding. These observations are consistent with the presence of the 3_{10}-helical conformation in solution because earlier literature suggests that the solvent exposure of only two N-terminal NH groups is indicative of a continuous 3_{10}-helical

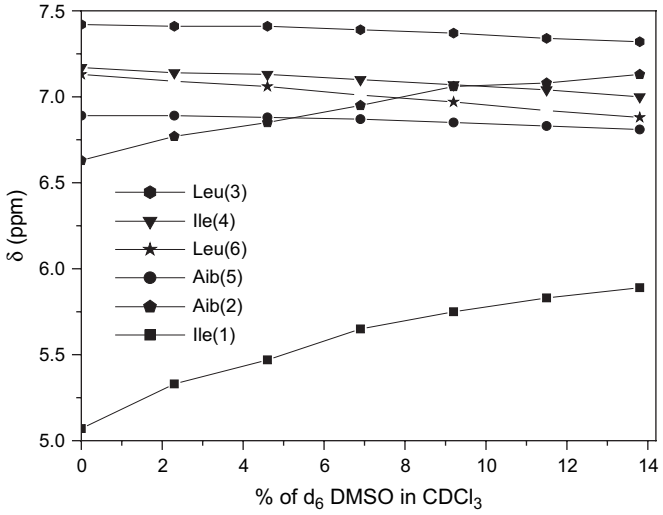

Figure 6. NMR solvent titration curve for NH protons in peptide **I**.

conformation.[9a,10] We are unable to characterize the solvent perturbation experiment of peptides **II** and **III** due to partial overlapping of the NH signals with the aromatic protons.

Further attempts to characterize the conformation in $CDCl_3$ using NOEs reveal that peptide **I** exhibits most of the NN(i, i+1) pattern, indicative of a helical conformation in solution. Moreover, the ROESY spectrum clearly shows a long range connectivity $d_{\alpha\,N}$ (i, i+2) [Ile(1)↔Leu(3); Leu(3)↔Aib(5); Ile(4)↔Leu(6)] (Fig. 7), diagnostic of a 3_{10}-helical conformation.[11] In an α-helix the $d_{\alpha\,N}$ (i, i+2) would be approximately 4.5 Å, whereas in the 3_{10}-helix the same separation is reduced to 3.7 Å. Therefore, only in a 3_{10}-helix can one expect to detect the $d_{\alpha\,N}$ (i, i+2) crosspeaks, although these will be of low intensity.[11] In this peptide the only $d_{\alpha\,N}$ (i, i+4) detectable NOE is that relating the Ile(1)$C^{\alpha}H$ proton to the Aib(5) NH proton. Since this interaction is not observed in Figure 7, it is reasonable to assume that the structure adopted by peptide **I** is a 3_{10} type.

The conformations of the peptides **I**–**III** were probed further in solution phase by far-UV CD measurements in acetonitrile. The CD patterns for peptides **I**–**III** are presented in Figure 8. Peptides **I** and **III** show a strong negative band centered at 204 nm, which is followed by a weak negative shoulder at about 225 nm. Generally in the right-handed α-helix the intensities of the two negative maxima at 208 nm (parallel component of the π→π* transition) and 222 nm (n→π* transition) are very close.[12] It is known that in the 3_{10}-helix the n→π* transition is expected to exhibit a drastically reduced intensity with respect to that of the π→π* transition and tends to undergo a modest blue shift.[13] Therefore, peptides

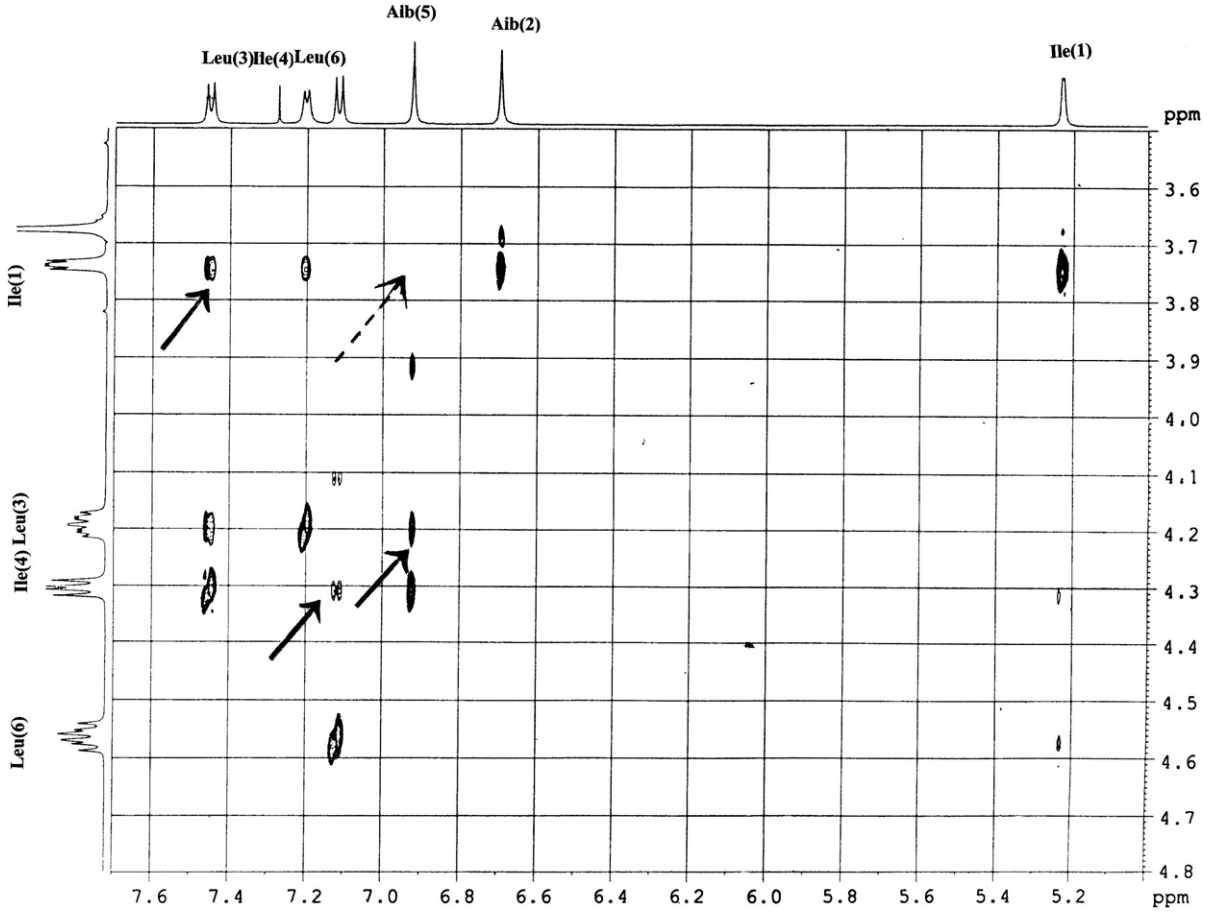

Figure 7. Section of the ROESY spectrum of peptide **I** in $CDCl_3$ (peptide concn: 1×10^{-2} M). The [$d_{\alpha\,N}$ (i, i+2), where i=1, 3, and 4] crosspeaks typical of a 3_{10}-helix are indicated (full arrow). The area in the spectrum where the undetected [$d_{\alpha\,N}$(i, i+4), where i=1] crosspeak typical of an α-helix was expected is also marked (dashed arrow).

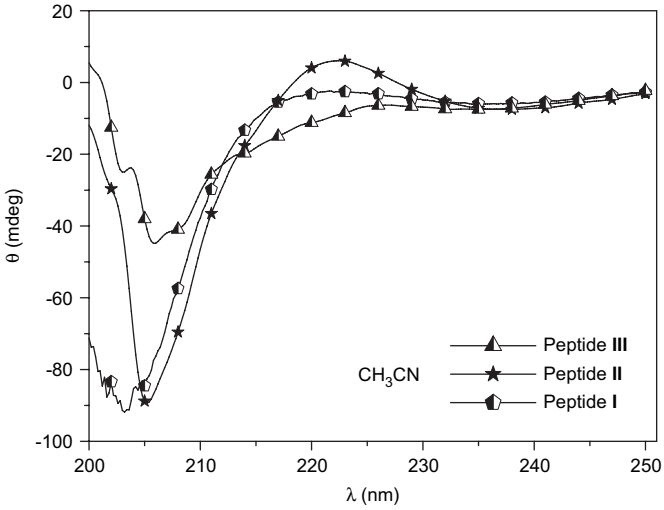

Figure 8. CD curves of peptides **I**–**III** in acetonitrile (1.5 mM).

I and **III** adopt 3_{10}-helical conformations in acetonitrile. Peptide **II** shows a weak positive shoulder at about 225 nm instead of a weak negative shoulder as it is observed in peptides **I** and **III** (Fig. 8), which may be due to some aggregation in acetonitrile. Nevertheless, the CD data strongly favor the conclusion that the three peptides **I**–**III** are folded into well-developed homogeneous 3_{10}-helical conformations in solution.

2.3. Morphological studies

It has been suggested that not only β-sheets but also helices have a significant role in amyloid fibril formation where the α-helices are stacked along the fibril axis.[14] Goldsbury et al. have suggested that for human amylin, α-helices may have a role in highly ordered self-aggregated amyloid plaque formation.[15] It is established that in the amyloidogenic peptide calcitonin ribbon-like structures twist back upon themselves to afford hollow tube-like assemblies.[16] Recently, several reports show that peptide based supramolecular helices also produce fibrillar structures through self-assembly.[17] Therefore, we became interested in exploring the possibility of fibril formation in peptides **I**–**III**. Field emission scanning electron microscopic (FE-SEM) images (10,000 times magnified) of the dried fibrous material of peptide **II** grown slowly from acetone clearly demonstrate that the aggregates in the solid state are bunches of non-twisted ribbon-like structures (Fig. 9a and 9b). It was observed that peptides **I** and **III** do not produce any fibrous material under similar conditions. Peptide **II** exhibits higher ordered self-assembly to generate ribbon-like structures. The supramolecular helices of **II** generated from primary building block helix (Fig. 5) aggregate through non-covalent interactions to form non-twisted filaments. The filaments can lead to ribbon-like assemblies through lateral association. Interestingly, the SEM images of **II** clearly demonstrate that the ribbon-like structures are formed through lateral association of non-twisted filaments (Fig. 9a and 9b). The regular parallel alignment of phenyl rings on the surface of supramolecular helices of peptide **II** (Fig. 5) probably helps in

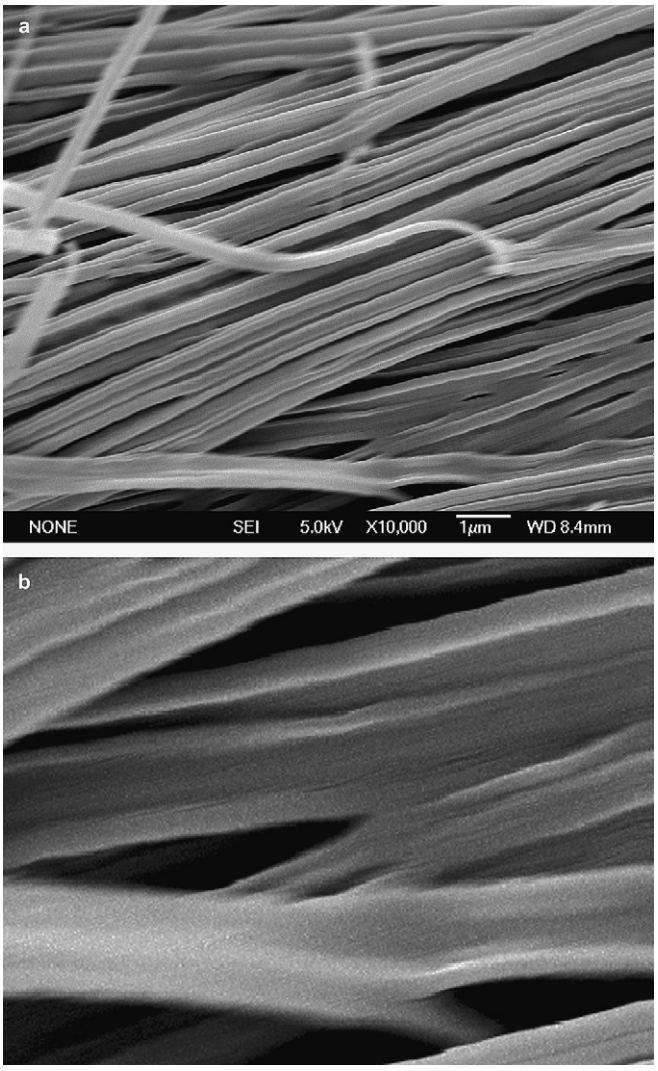

Figure 9. (a) FE-SEM image (×10,000) of peptide **II** showing the formation of non-twisted ribbon-like structures. (b) The enlarged SEM image clearly demonstrates that the ribbons are formed through lateral association of non-twisted filaments.

higher ordered self-assembly through non-covalent interactions, which is absent in peptides **I** and **III**. The quasi-crystalline structures of flat non-twisted morphology may be useful for specific nano-applications. Various attempts to fabricate these types of structures using amyloid proteins, peptides, and viruses have been reported.[18]

3. Conclusions

In peptides with lower Aib content (<50%), conformational heterogeneity is a common phenomenon. The present attempt to characterize the preferred conformations of the three designed hexapeptides containing Aib at positions 2 and 5 establishes that in the solid state they adopt mixed 3_{10}/α-helical conformations and in the solution phase well-developed homogeneous 3_{10} helical conformations. Because of considerable conformational flexibility, they attain different structures in different environments through conformational

transitions. It is reasonable to assume that hexapeptides with less than two Aib residues may facilitate α-helical conformations. The present study also reveals that hexapeptides cannot generate the helix-terminating Schellman motif unlike longer peptides when the achiral Aib is placed at the penultimate position from the C-terminus. In the crystalline state, the helices are packed in head-to-tail fashion through intermolecular hydrogen bonds to create supramolecular helical structures. It has been shown that peptide **II** can form ribbon-like structures that are generated through lateral association of non-twisted filaments. These quasi-crystalline structures of flat non-twisted morphology may find useful applications in nanotechnology. The results indicate that synthetic Aib-containing peptide helices can form highly ordered self-aggregated amyloid plaque like human amylin.[15]

4. Experimental

4.1. Synthesis of peptides

Peptides **I**–**III** were synthesized by conventional solution phase procedures using a racemization free, fragment condensation strategy (Scheme 1).[19] The *tert*-butyloxycarbonyl and methyl ester groups were used for amino and carboxyl protections, respectively, and dicyclohexylcarbodiimide (DCC) and 1-hydroxybenzotriazole (HOBT) as coupling agents. Deprotections were performed using trifluoroacetic acid or saponification, respectively. Methyl ester hydrochlorides of Aib, Leu, and Phe were prepared by the thionyl chloride–methanol procedure. All the intermediates obtained were checked for purity by thin layer chromatography (TLC) on silica gel and used without further purification. All the final peptides were purified by column chromatography using silica gel (100–200 mesh) as the stationary phase and ethyl acetate and petroleum ether mixture as the eluent. The reported peptides **I**–**III** were fully characterized by X-ray crystallography and NMR studies.

4.1.1. Boc–Ile–Aib–Leu–OH *1*

Boc–Ile–Aib–Leu–OMe[20] (1.1 g, 2.48 mmol) was dissolved in methanol (15 ml) and 2 M NaOH (10 ml) was added. The reaction mixture was stirred at room temperature for 2 days. The progress of the reaction was monitored by TLC. After completion of the reaction, methanol was evaporated. The residue obtained was diluted with water and washed with diethylether. The aqueous layer was cooled in ice and neutralized by 2 M HCl and extracted with ethyl acetate. The solvent was evaporated in vacuo to give a white solid.

Yield: 0.96 g (90.0%). Mp=118–120 °C; IR (KBr): 3419, 3315, 1667, 1523 cm^{-1}; ^1H NMR (300 MHz, DMSO-d_6, δ ppm): 7.90 (Aib(2) NH, 1H, s), 7.37 (Leu(3) NH, 1H, d, J=7.8 Hz), 6.76 (Ile(1) NH, 1H, d, J=7.5 Hz), 4.22–4.24 ($C^{\alpha}H$ of Leu(3), 1H, m), 3.73–3.77 ($C^{\alpha}H$ of Ile(1), 1H, m), 1.55–1.80 ($C^{\beta}Hs$ of Ile(1), Leu(3); $C^{\gamma}Hs$ of Leu(3); 4H, m), 1.38 (Boc–CH_3s, 9H, s), 1.35 ($C^{\beta}Hs$ of Aib, 6H, s), 1.06–1.11 ($C^{\gamma}Hs$ of Ile(1), 2H, m), 0.85–0.87 ($C^{\gamma}Hs$ of Ile(1), $C^{\delta}Hs$ of Ile(1), Leu(3), 12H, m). Anal. Calcd for $C_{21}H_{39}N_3O_6$ (429.54): C, 58.72; H, 9.15; N, 9.78. Found: C, 58.55; H, 8.98; N, 9.58.

4.1.2. Boc–Ile–Aib–Phe–OH *2*

Boc–Ile–Aib–Phe–OMe[20] (0.6 g, 1.26 mmol) was dissolved in methanol (15 ml) and 2 M NaOH (8 ml) was added. The reaction mixture was stirred at room temperature for 2 days. The progress of the reaction was monitored by TLC. After completion of the reaction, methanol was evaporated. The residue obtained was diluted with water and washed with diethylether. The aqueous layer was cooled in ice, neutralized by 2 M HCl, and extracted with ethyl acetate. The solvent was evaporated in vacuo to give a white solid.

Yield: 0.52 g (89.0%). Mp=108–110 °C; IR (KBr): 3415, 3314, 1666, 1523 cm^{-1}; ^1H NMR (300 MHz, DMSO-d_6, δ ppm): 7.87 (Aib(2) NH, 1H, s), 7.49 (Phe(3) NH, 1H, d, J=7.5 Hz), 7.18–7.28 (phenyl ring protons, 5H, m), 6.76 (Ile(1) NH, 1H, d, J=7.5 Hz), 4.40–4.42 ($C^{\alpha}H$ of Phe(3), 1H, m), 3.73–3.78 ($C^{\alpha}H$ of Ile(1), 1H, m), 2.89–3.06 ($C^{\beta}Hs$ of Phe(3), 2H, m), 1.66–1.68 ($C^{\beta}Hs$ of Ile(1), 1H, m), 1.37 (Boc–CH_3s, 9H, s), 1.28 ($C^{\beta}Hs$ of Aib(2), 6H, s), 1.05–1.10 ($C^{\gamma}Hs$ of Ile(1), 2H, m), 0.80–0.88 ($C^{\gamma}Hs$ and $C^{\delta}Hs$ of Ile(1), 6H, m). Anal. Calcd for $C_{24}H_{37}N_3O_6$ (463.56): C, 62.17; H, 8.04; N, 9.06. Found: C, 62.02; H, 7.89; N, 9.24.

4.1.3. Boc–Ile–Aib–Leu–Ile–Aib–Leu–OMe (peptide *I*)

To Boc–Ile–Aib–Leu–OMe[20] (0.52 g, 1.17 mmol), trifluoroacetic acid (5 ml) was added at 0 °C and stirred at room temperature. The removal of the Boc group was monitored by TLC. After 8 h, the trifluoroacetic acid was removed under reduced pressure to afford the crude trifluoroacetate salt. The residue was taken up in water and washed with diethylether. The pH of the aqueous solution was adjusted to 8 with sodium bicarbonate and extracted with ethyl acetate. The extracts were pooled, washed with saturated brine, dried over sodium sulfate, and concentrated to a highly viscous liquid that gave a positive ninhydrin test. This tripeptide free base was added to a well ice-cooled solution of **1** (0.50 g, 1.17 mmol) in DMF (4 ml) followed by DCC (0.26 g, 1.28 mmol) and HOBt (0.17 g, 1.28 mmol). The reaction mixture was stirred at room temperature for 4 days. The residue was taken up in ethyl acetate and dicyclohexylurea (DCU) was filtered off. The organic layer was washed with 2 M HCl (3×50 ml), 1 M Na_2CO_3 solution (3×50 ml), and brine, dried over anhydrous Na_2SO_4, and evaporated in vacuo to yield a white solid. Purification was done using silica gel as stationary phase and ethyl acetate–petroleum ether mixture as the eluent. Single crystals were grown from acetone–petroleum ether mixture by slow evaporation and were stable at room temperature.

Yield: 0.73 g (83.0%). Mp=178–180 °C; $[\alpha]_{589}^{20}$ −8.1 (*c* 0.10 g/100 ml, CH_3OH); IR (KBr): 3421, 3337, 1738, 1668 cm^{-1}; ^1H NMR (500 MHz, $CDCl_3$, δ ppm): 7.45 (Leu(3) NH, 1H, d, J=8.0 Hz), 7.20 (Ile(4) NH, 1H, d, J=6.0 Hz), 7.12 (Leu(6) NH, 1H, d, J=8.5 Hz), 6.92 (Aib(5) NH, 1H, s), 6.69 (Aib(2) NH, 1H, s), 5.22 (Ile(1) NH, 1H, d, J=2.5 Hz), 4.54–4.58 ($C^{\alpha}H$ of Leu(6), 1H, m), 4.29–

4.32 ($C^{\alpha}H$ of Ile(4), 1H, m), 4.18–4.21 ($C^{\alpha}H$ of Leu(3), 1H, m), 3.73–3.75 ($C^{\alpha}H$ of Ile(1), 1H, m), 3.68 ($-OCH_3$, 3H, s), 1.59–2.15 ($C^{\beta}Hs$ of Ile(1), Leu(3), Ile(4), and Leu(6), 6H, m), 1.56 ($C^{\beta}Hs$ of Aib(5), 6H, s), 1.53 ($C^{\beta}Hs$ of Aib(2), 6H, s), 1.48 (Boc–CH_3s, 9H, s), 1.25–1.30 ($C^{\gamma}Hs$ of Ile(1), Leu(3), Ile(4), and Leu(6), 6H, m), 0.87–1.0 ($C^{\gamma}Hs$ of Ile(1) and Ile(4); $C^{\delta}Hs$ of Ile(1), Ile(4), Leu(3), and Leu(6), 24H, m); ^{13}C NMR (75 MHz, $CDCl_3$, δ ppm): 174.86, 173.57, 173.31, 171.69, 171.03, 157.12, 81.32, 61.20, 59.29, 57.23, 56.69, 54.02, 51.87, 50.91, 40.99, 40.08, 36.14, 35.69, 30.87, 28.13, 27.83, 25.74, 25.47, 25.17, 24.95, 24.58, 23.28, 23.15, 22.97, 20.71, 15.78, 15.46, 11.70, 11.42. Anal. Calcd for $C_{38}H_{70}N_6O_9$ (754.98): C, 60.45; H, 9.34; N, 11.13. Found: C, 60.31; H, 9.23; N, 11.01.

4.1.4. Boc–Ile–Aib–Leu–Ile–Aib–Phe–OMe (peptide **II**)

Peptide Boc–Ile–Aib–Phe–OMe[20] (0.5 g, 1.05 mmol) was dissolved in trifluoroacetic acid (5 ml) at 0 °C and stirred at room temperature for 8 h. The work up of the free base was done as in the preparation of peptide **I**. The tripeptide free base was added to a well ice-cooled solution of **1** (0.45 g, 1.05 mmol) in DMF (4 ml) followed by DCC (0.24 g, 1.15 mmol) and HOBt (0.16 g, 1.15 mmol). After 4 days, the reaction mixture was worked up as reported in the case of peptide **I** to afford the peptide as a white solid. Purification was done using silica gel as stationary phase and ethyl acetate–petroleum ether mixture as the eluent. Single crystals were grown from acetone–petroleum ether mixture by slow evaporation and were stable at room temperature.

Yield: 0.71 g (86.0%). Mp=186–188 °C; $[\alpha]_{589}^{20}$ −16.4 (*c* 0.10 g/100 ml, CH_3OH); IR (KBr): 3421, 3366, 1738, 1671 cm^{-1}; ^1H NMR (300 MHz, $CDCl_3$, δ ppm): 7.48 (Leu(3) NH, 1H, d, *J*=7.5 Hz), 7.38 (Ile(4) NH, 1H, d, *J*=8.1 Hz), 7.17–7.26 (Phe(6) NH, phenyl ring protons 6H, m), 6.96 (Aib(5) NH, 1H, s), 6.69 (Aib(2) NH, 1H, s), 5.22 (Ile(1) NH, 1H, br s), 4.72–4.75 ($C^{\alpha}H$ of Phe(6), 1H, m), 4.25–4.29 ($C^{\alpha}H$ of Ile(4), 1H, m), 3.75–3.76 ($C^{\alpha}H$ of Leu(3), 1H, m), 3.70 ($-OCH_3$, 3H, s), 3.64–3.66 ($C^{\alpha}H$ of Ile(1), 1H, m), 3.12–3.13 ($C^{\beta}Hs$ of Phe(6), 2H, m), 1.60–1.88 ($C^{\beta}Hs$ of Ile(1), Ile(4), and Leu(3), 4H, m), 1.54 ($C^{\beta}Hs$ of Aib(5), 6H, s), 1.53 ($C^{\beta}Hs$ of Aib(2), 6H, s), 1.49 (Boc–CH_3s, 9H, s), 1.24–1.33 ($C^{\gamma}Hs$ of Ile(1), Leu(3), Ile(4), 5H, m), 0.85–0.97 ($C^{\gamma}Hs$ of Ile(1) and Ile(4); $C^{\delta}Hs$ of Ile(1), Ile(4), and Leu(3), 18H, m); ^{13}C NMR (75 MHz, $CDCl_3$, δ ppm): 174.69, 174.63, 173.53, 172.09, 171.38, 171.09, 157.05, 137.13, 129.34, 128.20, 126.49, 81.41, 60.98, 59.37, 57.21, 56.68, 54.03, 51.95, 40.11, 38.00, 36.30, 35.78, 28.12, 27.81, 26.07, 25.60, 24.97, 24.93, 24.61, 23.35, 23.13, 20.77, 15.74, 15.47, 11.65, 11.46. Anal. Calcd for $C_{41}H_{68}N_6O_9$ (789.00): C, 62.41; H, 8.68; N, 10.65. Found: C, 62.26; H, 8.52; N, 10.67.

4.1.5. Boc–Ile–Aib–Phe–Ile–Aib–Leu–OMe (peptide **III**)

Peptide Boc–Ile–Aib–Leu–OMe (0.53 g, 1.19 mmol) was dissolved in trifluoroacetic acid (5 ml) at 0 °C and stirred at room temperature for 8 h. The work up of the free base was done as in the preparation of peptide **I**. The tripeptide free base was added to a well ice-cooled solution of **2** (0.55 g, 1.19 mmol) in DMF (4 ml) followed by DCC (0.27 g, 1.31 mmol) and HOBt (0.16 g, 1.31 mmol). After 4 days, the reaction mixture was worked up as usual to afford the peptide as a white solid. Purification was done using silica gel as stationary phase and ethyl acetate–petroleum ether mixture as the eluent. Single crystals were grown from acetone–petroleum ether mixture by slow evaporation and were stable at room temperature.

Yield: 0.67 g (81.0%). Mp=192–194 °C; $[\alpha]_{589}^{20}$ −16.6 (*c* 0.10 g/100 ml, CH_3OH); IR (KBr): 3421, 3366, 1738, 1671 cm^{-1}; ^1H NMR (300 MHz, $CDCl_3$, δ ppm): 7.48 (Phe(3) NH, 1H, d, *J*=8.4 Hz), 7.20–7.31 (Ile(4) NH, phenyl ring protons 6H, m), 7.07 (Leu(6) NH, 1H, d, *J*=8.1 Hz), 6.88 (Aib(5) NH, 1H, s), 6.57 (Aib(2) NH, 1H, s), 5.14 (Ile(1) NH, 1H, d, *J*=3.9 Hz), 4.53–4.66 ($C^{\alpha}H$ of Phe(6), 1H, m), 4.43–4.46 ($C^{\alpha}Hs$ of Ile(4), 1H, m), 3.71–3.73 ($C^{\alpha}H$ of Leu(3), 1H, m), 3.67 ($-OCH_3$, 3H, s), 3.45–3.52 ($C^{\alpha}Hs$ of Ile(1), 1H, m), 3.0–3.1 ($C^{\beta}Hs$ of Phe(3), 2H, m), 1.60–1.90 ($C^{\beta}Hs$ of Ile(1), Ile(4), and Leu(6), 4H, m), 1.55 ($C^{\beta}Hs$ of Aib(5), 6H, s), 1.48 ($C^{\beta}Hs$ of Aib(2), 6H, s), 1.41 (Boc–CH_3s, 9H, s), 1.27–1.29 ($C^{\gamma}Hs$ of Ile(1), Ile(4) and Leu(6), 5H, m), 0.87–0.97 ($C^{\gamma}Hs$ of Ile(1), Ile(4); $C^{\delta}Hs$ of Ile(1), Ile(4), and Leu(6), 18H, m); ^{13}C NMR (75 MHz, $CDCl_3$, δ ppm): 174.80, 174.65, 173.25, 172.23, 172.21, 170.84, 157.00, 137.13, 128.47, 128.19, 126.64, 81.03, 60.87, 59.31, 57.151, 56.61, 55.48, 51.83, 50.81, 41.08, 36.53, 35.81, 28.06, 27.11, 25.42, 25.28, 24.58, 24.51, 23.10, 22.83, 21.66, 15.76, 15.41, 11.56, 11.20. Anal. Calcd for $C_{41}H_{68}N_6O_9$ (789.00): C, 62.41; H, 8.68; N, 10.65. Found: C, 62.30; H, 8.65; N, 10.55.

4.2. FTIR spectroscopy

IR spectra were examined using a Perkin Elmer-782 model spectrophotometer. The solid-state FTIR measurements were performed using the KBr disk technique.

4.3. NMR experiments

All ^1H and ^{13}C NMR studies were recorded on a Bruker Avance 300 model spectrometer operating at 300 and 75 MHz, respectively. The 2D experiment was carried out in $CDCl_3$ on a Bruker DRX 500 MHz equipped with a 5 mm broadband inverse probe head. The peptide concentrations were in the range 5–10 mM in $CDCl_3$ for ^1H NMR and 30–40 mM in $CDCl_3$ for ^{13}C NMR.

4.4. Circular dichroism spectroscopy

Solutions of peptides **I**–**III** in acetonitrile (1.5 mM as final concentration) were used for obtaining the spectra. Far-UV CD measurements were recorded at 25 °C with a 0.5 s averaging time, a scan speed of 50 nm/min, using a JASCO spectropolarimeter (J 720 model) equipped with a 0.1 cm path length cuvette. The measurements were taken at 0.2 nm wavelength

Table 4
Crystallographic refinement details for peptides **I**–**III**

	Peptide **I**	Peptide **II**	Peptide **III**
Formula	$C_{38}H_{70}N_6O_9$	$C_{41}H_{68}N_6O_9$	$C_{41}H_{68}N_6O_9$
MW	755.00	789.00	789.00
Crystal system	Monoclinic	Monoclinic	Trigonal
Cell dimensions [Å (°)]			
a	9.7556(13)	9.9545(7)	11.5100(5)
b	19.023(5)	18.5960(16)	11.5100(5)
c	11.8045(19)	11.9741(9)	28.5496(9)
α	(90)	(90)	(90)
β	91.258(12)	91.811(8)	(90)
γ	(90)	(90)	(120)
U/Å^3	2190.1(7)	2215.5(3)	3275.5(2)
D_{calcd} (g cm^{-3})	1.145	1.180	1.200
Unique reflections	11,250	11,008	7631
Reflections>2σ(*I*)	3072	4046	4503
*R*1 (all data)	0.2203	0.1304	0.1118
*wR*2 (all data)	0.1464	0.1663	0.1901
*R*1 (*I*>2σ(*I*))	0.0689	0.0696	0.0634
*wR*2 (*I*>2σ(*I*))	0.1203	0.1475	0.1558
Max, Min elec. density (e Å^{-3})	0.191, −0.206	0.339, −0.329	0.625, −0.365

intervals, 2.0 nm spectral bandwidth, and five sequential scans were recorded for each sample.

4.5. Field emission scanning electron microscopic study

Morphology of peptide **II** was investigated using field emission scanning electron microscope (FE-SEM). For the study, fibrous materials (slowly grown from acetone) were dried and gold coated. The micrograph was taken using a FE-SEM apparatus (JEOL JSM-6700F).

4.6. Single crystal X-ray diffraction study

Crystal data and refinement details are given in Table 4. Diffraction data for the three peptides **I**–**III** were obtained with Mo Kα radiation at 150 K using the Oxford Diffraction X-Calibur CCD System. The crystals were positioned at 50 mm from the CCD; 321 frames were measured with a counting time of 10 s. Data analyses were carried out with the Crysalis program.[21] The structures were solved using direct methods with the SHELXS-97 program.[22] The non-hydrogen atoms were refined with anisotropic thermal parameters. The hydrogen atoms bonded to carbon were included in geometric positions and given thermal parameters equivalent to 1.2 times those of the atom to which they were attached. Crystallographic details have been deposited at the Cambridge Crystallographic Data centre, reference CCDC 651726–651728.

Acknowledgements

A.D. would like to thank UGC, New Delhi, India for providing a senior research fellowship. The financial assistance of UGC, New Delhi is acknowledged [Major Research Project No. 32-190/2006 (SR)]. We thank EPSRC and the University of Reading, UK for funds for Oxford Diffraction X-Calibur CCD diffractometer. The use of NMR facility at Bose Institute, Kolkata is acknowledged.

Supplementary data

Supplementary data associated with this article can be found in the online version, at doi:10.1016/j.tet.2007.11.016.

References and notes

1. (a) Karle, I. L.; Balaram, P. *Biochemistry* **1990**, *29*, 6747–6756; (b) Toniolo, C.; Benedetti, E. *Trends Biochem. Sci.* **1991**, *16*, 350–353; (c) Marshall, G. R.; Hodgkin, E. E.; Langs, D. A.; Smith, G. D.; Zabrocki, J.; Leplawy, M. T. *Proc. Natl. Acad. Sci. U.S.A.* **1990**, *87*, 487–491; (d) Karle, I. L.; Flippen-Anderson, J. L.; Uma, K.; Balaram, P. *Curr. Sci.* **1990**, *59*, 875–885; (e) Venkatraman, J.; Shankaramma, S. C.; Balaram, P. *Chem. Rev.* **2001**, *101*, 3131–3152; (f) Shamala, N.; Nagaraj, R.; Balaram, P. *Biochem. Biophys. Res. Commun.* **1977**, *79*, 291–297; (g) Nagaraj, R.; Shamala, N.; Balaram, P. *J. Am. Chem. Soc.* **1979**, *101*, 16–20; (h) Toniolo, C.; Benedetti, E. *ISI Atlas Sci.: Biochem.* **1988**, *1*, 225–230; (i) Kaul, R.; Balaram, P. *Bioorg. Med. Chem.* **1999**, *7*, 105–117; (j) Aravinda, S.; Shamala, N.; Das, C.; Sriranjini, A.; Karle, I. L.; Balaram, P. *J. Am. Chem. Soc.* **2003**, *125*, 5308–5315; (k) Karle, I. L.; Flippen-Anderson, J. L.; Uma, K.; Balaram, H.; Balaram, P. *Proc. Natl. Acad. Sci. U.S.A.* **1989**, *86*, 765–769.
2. (a) Andreeto, E.; Peggion, C.; Crisma, M.; Toniolo, C. *Biopolymers* **2006**, *84*, 490–501; (b) Aubry, A.; Bayeul, D.; Bruckner, H.; Schiemann, N.; Benedetti, E. *J. Pept. Sci.* **1998**, *4*, 502–510; (c) Crisma, M.; Andreetto, E.; Zotti, M. D.; Moretto, A.; Peggion, C.; Formaggio, F.; Toniolo, C. *J. Pept. Sci.* **2007**, *13*, 190–205; (d) Kokkinidis, M.; Tsernoglou, D.; Bruckner, H. *Biochem. Biophys. Res. Commun.* **1986**, *136*, 870–875.
3. (a) Karle, I. L.; Flippen-Anderson, J. L.; Uma, K.; Balaram, P. *Biopolymers* **1989**, *28*, 773–781; (b) Kokkinidis, M.; Banner, D. W.; Tsernoglou, D.; Bruechner, H. *Biochem. Biophys. Res. Commun.* **1986**, *139*, 590–595; (c) Rai, R.; Aravinda, S.; Kanagarajadurai, K.; Raghothama, S.; Shamala, N.; Balaram, P. *J. Am. Chem. Soc.* **2006**, *128*, 7916–7928; (d) Datta, S.; Uma, M. V.; Shamala, N.; Balaram, P. *Biopolymers* **1999**, *50*, 13–22.
4. (a) Banerjee, A.; Datta, S.; Pramanik, A.; Shamala, N.; Balaram, P. *J. Am. Chem. Soc.* **1996**, *118*, 9477–9483; (b) Datta, S.; Shamala, N.; Banerjee, A.; Pramanik, A.; Bhattacharjya, S.; Balaram, P. *J. Am. Chem. Soc.* **1997**, *119*, 9246–9251.
5. (a) Aleman, C.; Subirana, J. A.; Perez, J. J. *Biopolymers* **1994**, *32*, 621–631; (b) Huston, S. E.; Marshall, G. R. *Biopolymers* **1994**, *34*, 75–90; (c) Basu, G.; Kitao, A.; Hirata, F.; Go, N. *J. Am. Chem. Soc.* **1994**, *116*, 6307–6315; (d) Rives, J. T.; Maxwell, D. S.; Jorgenson, W. L. *J. Am. Chem. Soc.* **1993**, *115*, 11590–11593; (e) Zhang, L.; Hermans, J. *J. Am. Chem. Soc.* **1994**, *116*, 11915–11921; (f) Bolin, K. A.; Millhauser, G. L. *Acc. Chem. Res.* **1999**, *32*, 1027–1033; (g) Mammi, S.; Rainaldi, M.; Bellanda, M.; Schievano, E.; Peggion, E.; Broxterman, Q. B.; Formaggio, F.; Crisma, M.; Toniolo, C. *J. Am. Chem. Soc.* **2000**, *122*, 11735–11736.
6. (a) Schellman, C. *Protein Folding*; Jaenicke, R., Ed.; Elsevier, Biochemical: North Holland, Amsterdam, 1980; pp 53–61; (b) Nagarajaram, H. A.; Sowdhamini, R.; Ramakrishnan, C.; Balaram, P. *FEBS Lett.* **1993**, *321*, 79–83; (c) Aurora, R.; Srinivasan, R.; Rose, G. D. *Science* **1994**, *264*, 1126–1130; (d) Rajashankar, K. R.; Ramakumar, S. *Protein Sci.* **1996**, *5*, 932–946; (e) Viguera, A. R.; Serrano, L. *J. Mol. Biol.* **1995**, *251*, 150–160; (f) Benedetti, E.; Di Blasio, B.; Pavone, V.; Pedone, C.; Santini, A.; Bavoso, A.; Toniolo, C.; Crisma, M.; Sartore, L. *J. Chem. Soc., Perkin Trans. 2* **1990**, 1829–1837; (g) Di Blasio, B.; Pavone, V.; Saviano, R.; Fattorusso, C.; Pedone, E.; Benedetti, E.; Crisma, M.; Toniolo, C. *Pept. Res.* **1994**, *7*, 55–59.

7. Cormack, P. A. G.; Sherrington, D. C.; Moore, B. D. *J. Mater. Chem.* **1997**, *7*, 1977–1983.
8. Strong, A. E. *Chem. Commun.* **1998**, 473–474.
9. (a) Vijayakumar, E. K. S.; Balaram, P. *Tetrahedron* **1983**, *39*, 2725–2731; (b) Awasthi, S. K.; Raghothama, S. R.; Balaram, P. *J. Chem. Soc., Perkin Trans. 2* **1996**, 2701–2706.
10. (a) Iqbal, M.; Balaram, P. *J. Am. Chem. Soc.* **1981**, *103*, 5548–5552; (b) Vijayakumar, E. K. S.; Balaram, P. *Biopolymers* **1983**, *22*, 2133–2140.
11. Wuthrich, K. *NMR of Proteins and Nucleic Acids*; Wiley: New York, NY, 1986; pp 192–196.
12. (a) Blout, E. R. *Polyamino Acids, Polypeptides and Proteins*; Stahmann, M. A., Ed.; The University of Wisconsin Press: Madison, WI, 1962; pp 275–279; (b) Fasman, G. D. *Poly-α-amino Acids*; Fasman, G. D., Ed.; Dekker: New York, NY, 1967; pp 499–604; (c) Beychok, S. *Poly-α-amino acids*; Fasman, G. D., Ed.; Dekker: New York, NY, 1967; pp 293–337.
13. (a) Manning, M. C.; Woody, R. W. *Biopolymers* **1991**, *31*, 569–586; (b) Toniolo, C.; Polese, A.; Formaggio, F.; Crisma, M.; Kamphuis, J. *J. Am. Chem. Soc.* **1996**, *118*, 2744–2745; (c) Yoder, G.; Polese, A.; Silva, R. A. G. D.; Formaggio, F.; Crisma, M.; Broxterman, Q. B.; Kamphuis, J.; Toniolo, C.; Keiderling, T. A. *J. Am. Chem. Soc.* **1997**, *119*, 10278–10285; (d) Toniolo, C.; Formaggio, F.; Tognon, S.; Broxterman, Q. B.; Kaptein, B.; Huang, R.; Setnicka, V.; Keiderling, T. A.; Mc Coll, I. H.; Hecht, L.; Barron, L. D. *Biopolymers* **2004**, *75*, 32–45.
14. Arvinte, T.; Cudd, A.; Drake, A. F. *J. Biol. Chem.* **1993**, *268*, 6415–6422.
15. (a) Goldsbury, C.; Goldie, K.; Pellaud, J.; Seelig, J.; Frey, P.; Muller, S. A.; Kistler, J.; Cooper, G. J. S.; Aebi, U. *J. Struct. Biol.* **2000**, *130*, 352–362; (b) Farris, W.; Mansourian, S.; Chang, Y.; Lindsley, L.; Eckman, E. A.; Frosch, M. P.; Eckman, C. B.; Tanzi, R. E.; Selkoe, D. J.; Guenette, S. *Proc. Natl. Acad. Sci. U.S.A.* **2003**, *100*, 4162–4167.
16. Bauer, H. H.; Aebi, U.; Haner, M.; Hermann, R.; Muller, M.; Arvinte, T.; Merkle, H. P. *J. Struct. Biol.* **1995**, *115*, 1–15.
17. (a) Haldar, D.; Maji, S. K.; Sheldrick, W. S.; Banerjee, A. *Tetrahedron Lett.* **2002**, *43*, 2653–2656; (b) Haldar, D.; Drew, M. G. B.; Banerjee, A.; Banerjee, A. *Tetrahedron Lett.* **2002**, *43*, 5465–5468; (c) Banerjee, A.; Maji, S. K.; Drew, M. G. B.; Haldar, D.; Banerjee, A. *Tetrahedron Lett.* **2003**, *44*, 699–702; (d) Maji, S. K.; Banerjee, A.; Drew, M. G. B.; Haldar, D.; Banerjee, A. *Tetrahedron Lett.* **2002**, *43*, 6759–6762; (e) Haldar, D.; Drew, M. G. B.; Banerjee, A. *Tetrahedron* **2006**, *62*, 6370–6378; (f) Das, A. K.; Banerjee, A.; Drew, M. G. B.; Ray, S.; Haldar, D.; Banerjee, A. *Tetrahedron* **2005**, *61*, 5027–5036.
18. (a) Hartgerink, J. D.; Beniash, E.; Stupp, S. I. *Science* **2001**, *294*, 1684–1688; (b) Sone, E. D.; Stupp, S. I. *J. Am. Chem. Soc.* **2004**, *126*, 12756–12757; (c) Shenton, W.; Douglas, T.; Young, M.; Stubbs, G.; Mann, S. *Adv. Mater.* **1999**, *11*, 253–256; (d) Scheibel, T.; Parthasarathy, R.; Sawicki, G.; Lin, X. M.; Jaeger, H.; Lindquist, S. L. *Proc. Natl. Acad. Sci. U.S.A.* **2003**, *100*, 4527–4532; (e) Meegan, J. E.; Aggeli, A.; Boden, N.; Brydson, R.; Brown, A. P.; Carrick, L.; Brough, A. R.; Hussain, A.; Ansell, R. J. *Adv. Funct. Mater.* **2004**, *14*, 31–37; (f) Mc Millan, R. A.; Paavola, C. D.; Howard, J.; Chan, S. L.; Zaluzec, N. J.; Trent, J. D. *Nat. Mater.* **2002**, *1*, 247–252; (g) Mao, C.; Flynn, C. E.; Hayhurst, A.; Sweeney, R.; Qi, J.; Georgiou, G.; Iverson, B.; Belcher, A. M. *Proc. Natl. Acad. Sci. U.S.A.* **2003**, *100*, 6946–6951.
19. Bodanszky, M.; Bodanszky, A. *The Practice of Peptide Synthesis*; Springer: New York, NY, 1984; pp 1–282.
20. Dutt, A.; Dutta, A.; Mondal, R.; Spencer, E. C.; Howard, J. A. K.; Pramanik, A. *Tetrahedron* **2007**, *63*, 10282–10289.
21. *Crysalis, v1*; Oxford Diffraction Ltd: Oxford, UK, 2005.
22. Sheldrick, G. M. *SHELXS-97 and SHELXL-97, Programs for Crystallography*; University of Göttingen: Göttingen, Germany, 1997.